

# A Multi-Scale Urban Atmospheric Dispersion Model for Emergency Management

MIAO Yucong<sup>1</sup>, LIU Shuhua<sup>\*1</sup>, ZHENG Hui<sup>1</sup>, ZHENG Yijia<sup>1</sup>, CHEN Bicheng<sup>2</sup>, and WANG Shu<sup>1</sup>

<sup>1</sup>*Department of Atmospheric and Oceanic Sciences, School of Physics, Peking University, Beijing 100871*

<sup>2</sup>*Department of Meteorology, The Pennsylvania State University, University Park, Pennsylvania 16802, USA*

(Received 23 December 2013; revised 7 March 2014; accepted 3 April 2014)

## ABSTRACT

To assist emergency management planning and prevention in case of hazardous chemical release into the atmosphere, especially in densely built-up regions with large populations, a multi-scale urban atmospheric dispersion model was established. Three numerical dispersion experiments, at horizontal resolutions of 10 m, 50 m and 3000 m, were performed to estimate the adverse effects of toxic chemical release in densely built-up areas. The multi-scale atmospheric dispersion model is composed of the Weather Forecasting and Research (WRF) model, the Open Source Field Operation and Manipulation software package, and a Lagrangian dispersion model. Quantification of the adverse health effects of these chemical release events are given by referring to the U.S. Environmental Protection Agency's Acute Exposure Guideline Levels. The wind fields of the urban-scale case, with 3 km horizontal resolution, were simulated by the Beijing Rapid Update Cycle system, which were utilized by the WRF model. The sub-domain-scale cases took advantage of the computational fluid dynamics method to explicitly consider the effects of buildings. It was found that the multi-scale atmospheric dispersion model is capable of simulating the flow pattern and concentration distribution on different scales, ranging from several meters to kilometers, and can therefore be used to improve the planning of prevention and response programs.

**Key words:** WRF model, OpenFOAM, AEGLs, multi-scale simulation

**Citation:** Miao, Y. C., S. H. Liu, H. Zheng, Y. J. Zheng, B. C. Chen, and S. Wang, 2014: A multi-scale urban atmospheric dispersion model for emergency management. *Adv. Atmos. Sci.*, **31**(6), 1353–1365, doi: 10.1007/s00376-014-3254-9.

## 1. Introduction

In 1984, an accidental release of methyl isocyanate from a chemical plant happened in Bhopal, India (Bowonder and Miyake, 1988). In 1995, an intentional release of Sarin (GB) in a chemical attack on a Tokyo subway caused 12 deaths and affected thousands of people in Japan (Okumura et al., 1996). In 2005, an explosion event happened in a chemical plant in Jilin, China (Fu et al., 2008). Such events have increased concerns of governments regarding how to protect the public against accidental or malicious intentional release, especially in densely populated urban regions.

To plan appropriate response programs for emergency management, it is necessary to set up criteria to determine the severity and range of symptoms expected from the release. Therefore, the Acute Exposure Guideline Levels (AEGLs) program has been put into operation by the Environmental Protection Agency (EPA) since the 1990s. To date, the values of hundreds of toxic chemicals established under the AEGLs have been published by the EPA, and more will be addressed in the future. For further details regarding the AEGLs, read-

ers are referred to the following website: <http://www.epa.gov/oppt/aegl/index.htm>.

Three category levels of airborne concentration (ppm or  $\text{mg m}^{-3}$ ) are proposed by the EPA under the AEGLs, corresponding to increasingly severe adverse effects: notable discomfort (AEGL-1); serious health effects (AEGL-2); and life threatening effects (AEGL-3). For each AEGLs level, five exposure durations are given: 10 minutes, 30 minutes, 60 minutes, 240 minutes, and 480 minutes. The AEGLs have been widely employed in emergency management and response programs (Stage, 2004; Li et al., 2010; Acuesta et al., 2011), and are also used in the Areal Locations of Hazardous Atmospheres (ALOHA) model developed by the EPA and the National Oceanic and Atmospheric Administration (NOAA).

As the toxicological index has been given by the EPA, the exposure risk of hazardous chemicals for a specific region can be calculated using atmospheric dispersion models. Gaussian and box models, such as ALOHA, which are able to calculate results quickly, are widely employed for risk analysis. However, these models cannot explicitly take buildings into account, and it may be inappropriate to rely solely on these models to handle the emergency issues of urban areas, since the flow patterns of regions with buildings are quite dif-

\* Corresponding author: LIU Shuhua  
Email: lshuhua@pku.edu.cn

ferent from regions without the influence of buildings (Baik et al., 2009; Miao et al., 2013), as well as differences existing in the concentration distribution. Therefore, it is necessary to use high resolution models that can resolve buildings explicitly to help handle emergency management issues in densely built-up areas. For instance, Computational Fluid Dynamics (CFD) models are accurate enough for the detection of individual buildings, making them a useful tool for understanding 3D flow fields and associated concentration distributions within complex urban settings (Fitch et al., 2003).

The rapid increase of computing power and the development of more efficient methods in CFD models make it possible to use such methods to study the complex environmental and emergency problems within urban areas at high resolutions (Li et al., 2007; Baik et al., 2009; Hanna et al., 2009; Tewari et al., 2010; Miao et al., 2013).

In the present study, we established a multi-scale atmospheric model for emergency management, which is composed of a mesoscale model, a CFD model, and a dispersion model. This multi-scale model was used to evaluate the hazardous levels of a specific toxic chemical released in a built-up area by referring to the EPA-defined AEGLs values. The remainder of the paper is organized as follows. In section 2, the components of the multi-scale model are described. In section 3, the dispersion model is validated against a wind-tunnel experiment. Numerical experiments on three hypothetical intentional hazardous chemical releases on different scales are presented in section 4, with the discussion and conclusions given in section 5. To examine if the multi-scale urban atmospheric dispersion model can be used as practical tool for real-time emergency management, the forecasts of the real-time Beijing rapid update cycle (BJ-RUC) system were also used in the three numerical experiments.

## 2. Model descriptions

The multi-scale urban atmospheric dispersion model established in this study consists of a mesoscale model, a CFD model, and a Lagrangian dispersion model. The urban scale, defined by Fang et al. (2004), gives a horizontal resolution from tens of kilometers to hundreds of kilometers, and the buildings are parameterized to be implicitly resolved. The horizontal dimension of the sub-domain scale (Miao et al., 2006) is several kilometers, and the buildings are explicitly resolved. The prediction of the air flow on the urban scale can be simulated by using a mesoscale model, while the simulation of the sub-domain scale needs to take advantage of CFD models (Fitch et al., 2003; Chen et al., 2013).

### 2.1. Mesoscale model for urban-scale simulation

The mesoscale model used here is the Weather Research and Forecasting (WRF) model. The WRF model is used to simulate the wind and turbulence fields on the urban scale. The WRF-simulated results can be used to drive the dispersion model directly for the urban-scale numerical case, or provide the boundary conditions for the CFD model to re-

calculate the flow fields for the sub-domain-scale simulation (Miao et al., 2013).

To examine if the multi-scale urban atmospheric dispersion model can be used for real-time emergency management, the forecasts of the real-time BJ-RUC system are used in this study. The BJ-RUC system includes the WRF model and the WRF 3DVAR system and has been in operation at the Beijing Meteorological Bureau since June 2008 (Wang et al., 2013). Two one-way nested computational grids are employed in the BJ-RUC system, with horizontal grid spacing of 9 and 3 km, and horizontal grid dimensions of 649 (zonal)  $\times$  400 (meridional) and 550 (zonal)  $\times$  424 (meridional), respectively (Fig. 1a). There are 38 full eta levels from the surface to the 50 hPa level in the vertical direction and 10 levels below the height of 600 m that were used to provide the boundary conditions for the CFD simulation. Conventional data, such as radiosondes, synops, aircraft reports, global positioning system precipitable water, and high-frequency measurements from the Automatic Weather Station (AWS) network maintained by the Beijing Meteorological Bureau have been incorporated into the BJ-RUC system by the WRF 3DVAR since 2008 (Wang et al., 2013). A 3-hourly rapid update cycling is run in the 3 km inner domain (Fig. 1b) to improve the prediction in the 1 to 6 hour forecast range.

The regular procedure of the BJ-RUC system is as follows. First, two 72-h forecasts of the outer domain, with the initial and boundary fields interpolated from the National Centers for Environmental Prediction (NCEP) Global Forecast System (GFS)  $1^\circ \times 1^\circ$  analyses and forecasts are made at 0000 and 1200 UTC each day to provide the boundary conditions for the inner domain. Then, eight 24-h forecasts of the inner domain are made with a 3-h interval each day from 0000 to 2100 UTC. This is initiated by the real-time 3DVAR analysis with the first estimate from the previous 3-h inner domain simulation. The 3-h forecast from the current inner domain simulation will also provide the first estimation for the next simulation.

### 2.2. CFD model for sub-domain-scale simulation

As with the CFD model, version 2.1.1 of the Open Source Field Operation and Manipulation (OpenFOAM) software package is used. For further details of OpenFOAM, readers are referred to <http://www.openfoam.com>.

In this study, the simpleFoam solver, one of the standard solvers of OpenFOAM, is used to calculate the Reynolds-averaged Navier–Stokes (RANS) equations. Calculations are made with the standard  $k-\epsilon$  turbulence model by using the Semi-Implicit Method for Pressure-Linked Equations (SIMPLE) scheme (Ferziger and Peric, 2001). The SIMPLE scheme is an iterative method to solve the algebraic system of equations. A termination criterion of  $10^{-4}$  is used for all field variables in this study. The iterative procedure of the SIMPLE method is briefly introduced as follows:

Step 1: Set up the initial guess fields of pressure and velocity.

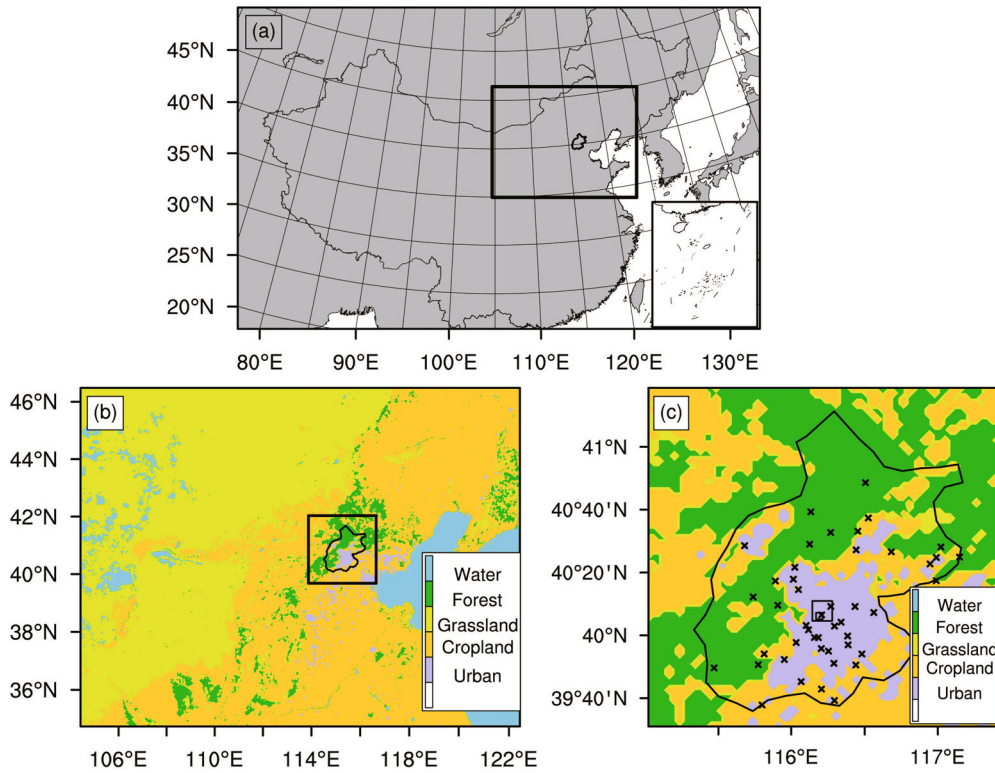


**Fig. 1.** (a) The model domains of BJ-RUC, and the land use category of (b) the inner domain of BJ-RUC and (c) the computational domain of the urban-scale numerical experiment. The black rectangle in (a) indicates the inner domain of BJ-RUC, and the black rectangle in (b) shows the extra computational domain of the urban-scale numerical experiment. The crosses in (c) show the locations of the 46 meteorological observations, and the two open squares in (c) indicate the computational domains of the two sub-domain numerical cases.

Step 2: Solve the momentum equation to compute the intermediate velocity field.

Step 3: Solve the pressure equation.

Step 4: Correct the velocities on the basis of the new pressure field.

Step 5: Update the guess fields of pressure and velocity.

Step 6: Repeat Step 2 to 5 until convergence.

For a specific numerical simulation case, the boundary conditions of wind velocity, turbulent kinetic energy (TKE) and its dissipation rate are provided directly or parameterized by using the results of the WRF model or other mesoscale models (Li et al., 2007; Baik et al., 2009; Tewari et al., 2010; Miao et al., 2013). In this study, the WRF–OpenFOAM coupled model (Miao et al., 2013) is used to predict the sub-domain-scale flow fields.

### 2.3. Dispersion model

After predicting wind and turbulence fields by using the WRF model or WRF–OpenFOAM coupled model, a Lagrangian dispersion model is used to simulate the concentration patterns of toxic chemicals on different scales over urban regions.

The Lagrangian dispersion model tracks transiently a large number of particles relative to wind flow to obtain the distribution of particles (Wilson and Sawford, 1996). The tra-

jectory of a Lagrangian particle can be expressed as

$$\mathbf{r}(t + \Delta t) = \mathbf{r}(t) + \mathbf{v}(\mathbf{r}, t)\Delta t, \quad (1)$$

$$\mathbf{v} = \mathbf{v}_m + \mathbf{v}', \quad (2)$$

where  $t$  is time,  $\Delta t$  is the time increment,  $\mathbf{r}$  is the position vector and  $\mathbf{v}$  is the wind vector. The wind vector is composed of two parts: the mean velocity component ( $\mathbf{v}_m$ ) and the turbulent velocity component ( $\mathbf{v}'$ ). The mean velocity component is directly used to generate the simulated results of WRF or OpenFOAM, while the turbulent velocity component needs to be parameterized. The turbulent motions (i.e.,  $u'$ ,  $v'$  and  $w'$ ) are assumed to be a Markov process (Stohl et al., 2005) and parameterized by two parameters: the Lagrangian timescale ( $T_{Li}$ ) and the turbulent velocity standard deviation ( $\sigma_i$ ).

At the different scales (i.e., the urban scale or sub-domain scale), the parameterized schemes of  $T_{Li}$  and  $\sigma_i$  are different. For the urban scale, the parameterized scheme of the Flexible Particle (FLEXPART) dispersion model (Stohl et al., 2005) is used. This utilizes the atmospheric boundary layer (ABL) parameters of the WRF-simulated result, such as the ABL height, Monin–Obukhov length, convective velocity scale, roughness length, and friction velocity.

For the sub-domain scale, since the TKE and its dissipation rate can be calculated by the CFD method,  $T_{Li}$  and  $\sigma_i$  are

directly parameterized by the TKE and dissipation rate (Wilson and Sawford, 1996; Zhang and Chen, 2007; Santiago and Martin, 2008):

$$\sigma_i^2 = \frac{2}{3}k, \quad (3)$$

$$T_{Li} = C_L \frac{k}{\varepsilon}, \quad (4)$$

where  $k$  and  $\varepsilon$  are the TKE and its dissipation rate, and the constant  $C_L$  is set to 0.3 (Berrouk et al., 2008).

#### 2.4. Determination of AEGLs values for the dispersion model

After simulating the concentration fields by the dispersion model, the toxic range and severity levels are calculated using the method proposed by Stage (2004), according to the EPA-defined AEGLs values. Three levels of severity for airborne concentrations are published by the EPA under the AEGLs, corresponding to increasingly severe adverse effects: notable discomfort (AEGL-1); serious health effects (AEGL-2); and life threatening effects (AEGL-3). For each level, five exposure durations are given: 10 minutes, 30 minutes, 60 minutes, 240 minutes, and 480 minutes. The procedure of the Stage (2004) method is briefly introduced as follows.

Step 1: Convert the simulated concentration fields,  $C$ , to the dosage fields,  $d$ :

$$d(x,y,z) = \sum_{n=1}^N \left( \frac{C(x,y,z,n-1) + C(x,y,z,n)}{2} \times \Delta t \right), \quad (5)$$

where  $d$  is the dosage ( $\text{ppm min}^{-1}$ ),  $C$  is the simulated concentration (ppm),  $\Delta t$  is the output interval (min), and  $N$  is the total number of concentration outputs in the temporal dimension.

Step 2: Calculate the effective exposure duration,  $T_{\text{eff}}$ :

$$T_{\text{eff}}(x,y,z) = \frac{d(x,y,z)}{C_{\max}(x,y,z)}, \quad (6)$$

where  $C_{\max}$  is the peak concentration (ppm) of the exposure period at each grid point, and  $T_{\text{eff}}$  is the effective exposure duration (min).

Step 3: Calculate the effective dosage,  $D_{\text{eff}}$ :

For  $T_{\text{eff}} < 480$  minutes,

$$D_{\text{eff}}(x,y,z,i) = D(k,i) \times \left( \frac{T_{\text{eff}}(x,y,z)}{T(k)} \right)^{A(k,i)+1}, \quad (7)$$

$$A(k,i) = \frac{\ln(D(k+1,i)/D(k,i))}{\ln(T(k+1)/T(k))} - 1, \quad (8)$$

where  $D_{\text{eff}}$  is the effective dosage ( $\text{ppm min}^{-1}$ );  $D(k,i)$  is the published AEGLs dosage ( $\text{ppm min}^{-1}$ ) for the  $i$ th ( $i = 1, 2, 3$ ) severity level of the  $k$ th ( $k = 1, 2, 3, 4, 5$ ) duration;  $T$  is the exposure duration of the published AEGLs (10 minutes, 30 minutes, 60 minutes, 240 minutes and 480 minutes); and when  $T_{\text{eff}} < 10$  minutes, the  $D(k,i)$  and  $A(k,i)$  of the 1st and 2nd durations (10 and 30 minutes) are used to calculate the  $D_{\text{eff}}$ .

For  $T_{\text{eff}} \geq 480$  minutes,

$$D_{\text{eff}}(x,y,z,i) = D(5,i). \quad (9)$$

Step 4: Compare the dosage,  $d$ , obtained in Step 1 at each location to the effective dosages,  $D_{\text{eff}}$ , obtained in Step 3, and calculate the AEGLs values,  $F$ , for each grid point.

For  $d(x,y,z) \leq D_{\text{eff}}(x,y,z,1)$ ,

$$F(x,y,z) = \frac{d(x,y,z)}{D_{\text{eff}}(x,y,z,1)}. \quad (10)$$

For  $D_{\text{eff}}(x,y,z,i) \leq d(x,y,z) \leq D_{\text{eff}}(x,y,z,i+1)$ ,

$$F(x,y,z) = i + \frac{d(x,y,z) - D_{\text{eff}}(x,y,z,i)}{D_{\text{eff}}(x,y,z,i+1) - D_{\text{eff}}(x,y,z,i)}. \quad (11)$$

For  $d(x,y,z) \geq D_{\text{eff}}(x,y,z,3)$ ,

$$F(x,y,z) = 3 + \frac{d(x,y,z) - D_{\text{eff}}(x,y,z,3)}{D_{\text{eff}}(x,y,z,3)}. \quad (12)$$

### 3. Validation of the dispersion model

In this section, a comprehensive wind-tunnel experimental dataset established by Thompson (1993) in the EPA wind-tunnel is used to validate the Lagrangian dispersion model. The wind-tunnel experimental dataset includes measurements of ground-level centerline normalized concentrations for various combinations of building shapes, emission stack heights, and emission stack locations relative to the building. The dataset was sorted by the National Environmental Research Institute of Denmark into a few Excel workbooks with embedded graphs and macros. For more details of the wind-tunnel experiment dataset, readers are referred to the study of Thompson (1993) and the atmospheric dispersion Wiki, available online at [http://atmosphericdispersion.wikia.com/wiki/Thompson\\_Wind\\_Tunnel\\_data](http://atmosphericdispersion.wikia.com/wiki/Thompson_Wind_Tunnel_data).

The wind-tunnel study designed by Thompson (1993) was designed for a point-source release of non-buoyant material in different positions near isolated rectangular buildings at a scale of 1 : 200. All the rectangular building shapes were placed in the same neutral atmospheric boundary layer, under the perpendicular approach flow condition. Two wind-tunnel experiments with different width buildings were used for validation, with both experiments constituting a  $0.5H$  (height of building) height stack located in front of the isolated building and a distance of  $2H$ . The difference between the two experiments was that one was a cubic building and the other was a  $2H$  wide rectangular building in the direction perpendicular to the wind direction.

To replicate the wind-tunnel experiment, the inflow conditions (velocity, TKE and its dissipation rate) were defined using the measurements of the actual wind-tunnel experiments, and the zero-gradient boundary condition was employed at the outflow boundaries (include the top boundary). The building surface was set as being in a no-slip condition and the wall turbulence functions (Chen et al., 2013) were

employed to the grid points adjacent to the walls. The computational domain of OpenFOAM was built by using the hexahedral elements, with a size of  $13H \times 11H \times 4H$  in the three dimensional direction (i.e.,  $X$ ,  $Y$ , and  $Z$ , respectively). For the horizontal dimension, the grid spacings were set to  $1/10H$ ; and in the vertical direction, the elements above and below the  $2H$  height were set to  $1/6H$  and  $1/10H$ , respectively. The number of computational cells was 457 600.

After simulating the OpenFOAM and the Lagrangian dispersion model the flow and concentration fields of the two wind-tunnel experiments were obtained (Fig. 2). The tracer particles were emitted continuously from the point-source at the location of ( $X = -2H$ ,  $Y = 0H$ ,  $Z = 0.5H$ ), and the concentration field was in steady state after integrating 600 steps with a one-second resolution. To compare with measurements, the simulated concentration was normalized by

$$C_{\text{norm}} = \frac{C_s u_H H^2}{Q}, \quad (13)$$

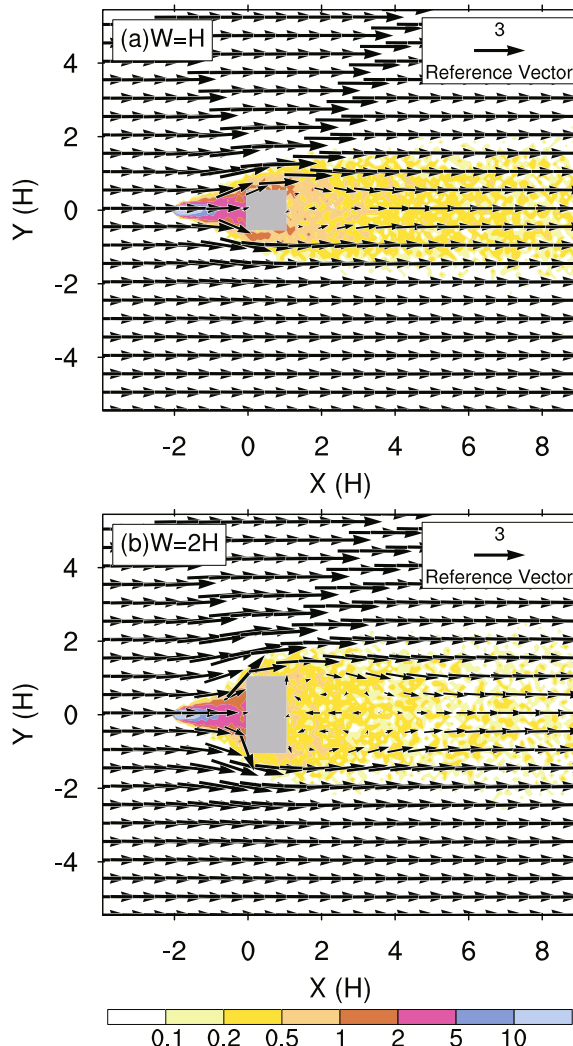


**Fig. 2.** The simulated wind vector fields and normalized concentration fields at the height of  $0.5H$ : (a) cubic building case; (b)  $2H$  wide rectangular building case.

where  $C_{\text{norm}}$  is the normalized concentration,  $C_s$  is the simulation concentration (ppm),  $u_H$  ( $\text{m s}^{-1}$ ) is the free stream velocity at the height of the building, and  $Q$  is the source strength ( $\text{m}^3 \text{s}^{-1}$ ).

Figure 2 illustrates the simulated wind vector fields and the normalized concentration fields at the height of  $0.5H$ , and it was found that a reversed circulated zone was formed on the leeward side of the building. The wider the building, the larger the size of the reversed zone formed.

A comparison of the measurements and the simulated dispersion is given in Fig. 3. For the cubic building case, despite the fluctuations of the simulated concentrations on the leeward side of the building ( $X > 1H$ ), the simulations were in good agreement with the measurements along the centerline (Fig. 3a). For the wider building case, the simulation of peak concentration ( $X = -0.5H$ ) on the windward side of the building was overestimated, as well as the simulated concentrations on the leeward side of the building (Fig. 3b). Despite this overestimation, the variation of the simulated concentration along the centerline was consistent with that of the measurement.

From this preliminary validation, it is concluded that the OpenFOAM-dispersion coupled model used in this study performs well in predicting the concentration distribution around a single building. More validations of OpenFOAM can be found in the previous studies by Miao et al. (2013, 2014).

#### 4. Numerical experiments of the multi-scale dispersion model

In this part of the study, three numerical experiments on hypothetical and intentional hazardous chemical releases, on

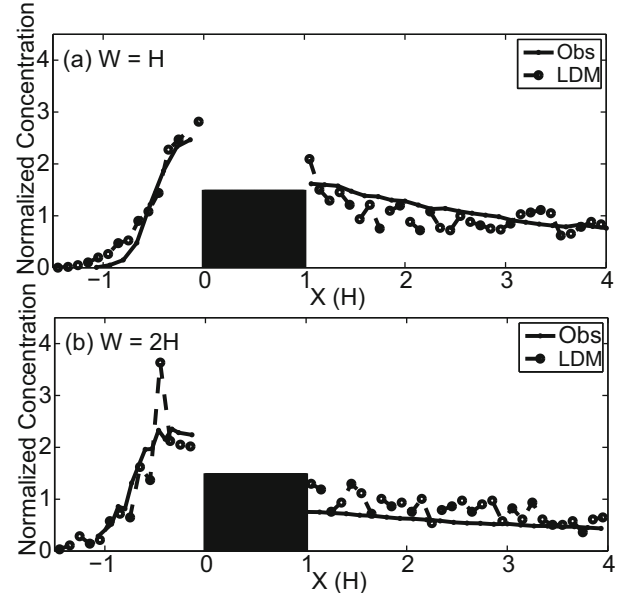


**Fig. 3.** The normalized concentration on the ground across the centerline ( $Y = 0H$ ): (a) cubic building case; (b)  $2H$  wide regular building case. Obs: observations of wind-tunnel experiment; LDM: simulations of the Lagrangian dispersion model. The black box indicates the location of the building along the centerline.

different scales, were performed. These were run using the real-time inner-domain simulation of the BJ-RUC system, at 0300 UTC (1100 LST) on 23 May 2013.

For the urban-scale numerical experiment, the simulations of the inner domain of the BJ-RUC system were directly employed to drive the Lagrangian dispersion model. For the sub-domain scale, the OpenFOAM model was first driven to recalculate the wind and turbulent fields by using the results of the BJ-RUC system, and then the dispersion processes were simulated using the Lagrangian dispersion model.

Details of the numerical experiments are given in Table 1. The sample toxic chemical used was Piperidine, one of the hazardous chemicals published by the EPA (Table 2). This was used as an example to illustrate the hazard evaluation procedure for emergency management. Piperidine is a widely used building block and chemical reagent in the synthesis of organic compounds. The emission rate given here is the effective gas release rate ( $\text{m}^3 \text{ s}^{-1}$ ).

#### 4.1. The urban-scale numerical experiment

##### 4.1.1. The real-time forecasts of the BJ-RUC system

The computational domain of the urban-scale numerical experiment is shown in Fig. 1c, which covers Beijing and its surrounding region. As shown in Table 1, the urban-scale numerical experiment was run from 1400 LST to 1600 LST 23 May 2013, i.e., from the third to the fifth hour from the simulated start time of 1100 LST.

The simulation of the 10 m wind and 2 m temperature fields during the studied period over the computational domain of the BJ-RUC system are given in Fig. 4. During the studied period, the southern wind dominated the Beijing area (Figs. 4a and 4c). In comparison to the observations, it was found that simulation overestimated the wind speed and the actual wind directions were more complicated (Fig. 4b and 4d). This was unlike the simulated consistent wind fields. Despite this inconsistency of the wind direction, the southern

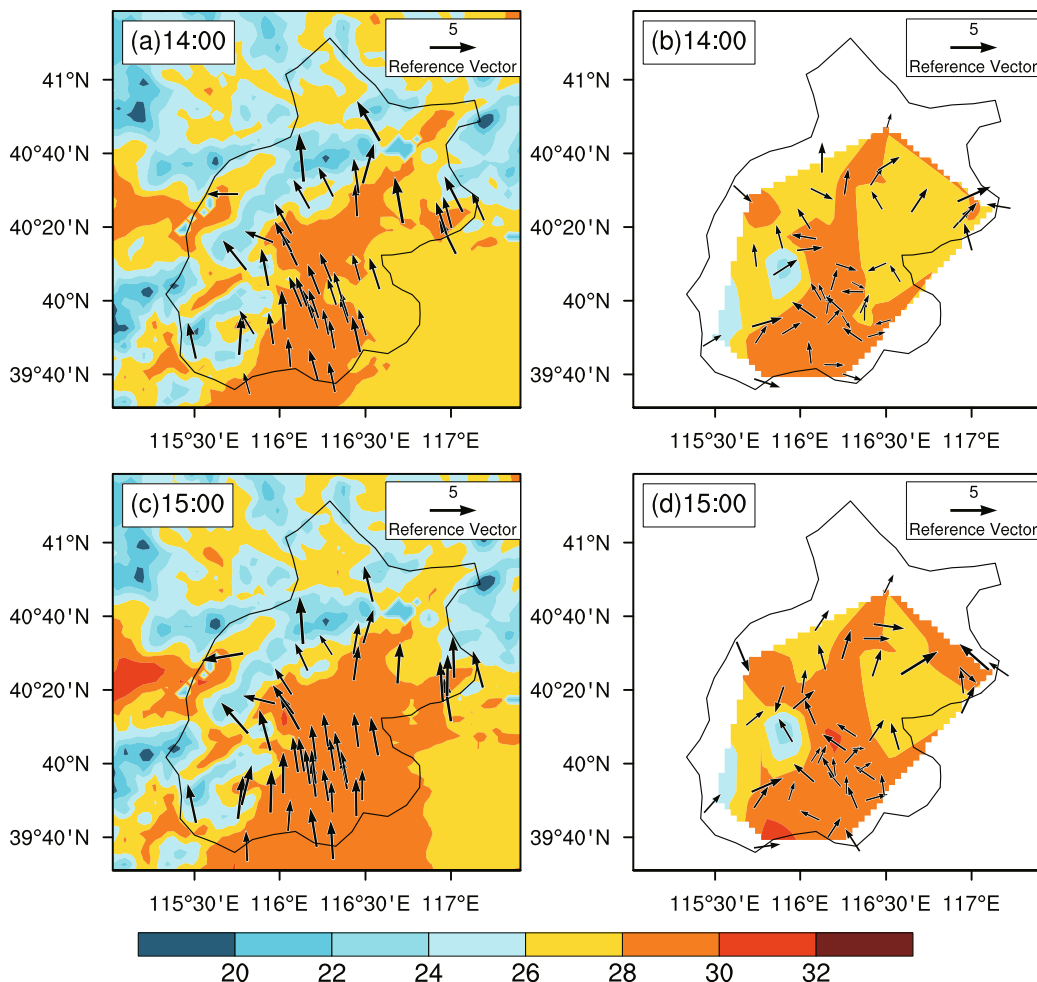


**Fig. 4.** The 10 m wind vectors fields ( $\text{m s}^{-1}$ ) and 2 m temperature fields ( $^{\circ}\text{C}$ ) of Beijing on 23 May 2013: (a) simulation of BJ-RUC at 1400 LST; (b) observation at 1400 LST; (c) simulation of BJ-RUC at 1500 LST; (d) observation at 1500 LST. Only the wind vectors of the grids nearest to the 46 stations are plotted here, and the measured 2-m temperature fields are interpolated by observations from the 46 stations. The measured wind speed and direction used here are the average values of the 10-minute record.

**Table 1.** Details of the dispersion numerical experiments.

Scale	Horizontal Resolution	Start Time	End Time	Time step (s)	Emission rate ( $\text{m}^3 \text{s}^{-1}$ )
Urban scale	3 km	1400 LST	1600 LST	60	50
Sub-domain	50 m	1400 LST	1500 LST	30	0.3
Sub-domain	10 m	1400 LST	1500 LST	10	0.03

**Table 2.** EPA-defined AEGLs values for Piperidine.

Exposure Time (min)	AEGL-1 (ppm)	AEGL-2 (ppm)	AEGL-3 (ppm)
10	10	50	370
30	10	50	180
60	6.6	33	110
240	2.6	13	45
480	1.7	8.3	28

wind components can be determined in most stations at 1400 and 1500 LST and the general condition of the wind fields can be predicted by the BJ-RUC system. The difference between the simulated and observed wind fields may be due to the simulated urban scale used here. The simulation can only resolve the air movements whose scales were larger than the grid spacing (i.e., 3 km), while the actual wind fields are the combinations of all the movement. Despite numerous observations being used to update the initial conditions, it was found to be impossible to predict the actual measurements on this scale. Fortunately, when we study the urban-scale dispersion processes, what dominates the concentration patterns is the “general air flow condition” that can be resolved.

However, it is rare that an emergency accident can affect a region up to  $10 \times 10 \text{ km}^2$ . Most emergency events are sub-domain scale cases, which need to be specially simulated using CFD models to resolve the sub-domain-scale movement of the air flow.

For the simulation of the 2 m temperature field, it was found that the simulated temperature fields were in good agreement with the observations (Fig. 4), especially in the center of Beijing where the density of stations is high.

#### 4.1.2. The urban-scale dispersion simulation and hazard evaluation

Four point sources were hypothetically set at ground level in the center of the built-up regions of Beijing ( $39.98^\circ\text{--}40.01^\circ\text{N}$ ,  $116.30^\circ\text{--}116.33^\circ\text{E}$ ), which were set to continuously emit during the simulation period. After simulating wind flow patterns using the BJ-RUC system, the concentration fields could be calculated in minutes by the Lagrangian dispersion model, which is quick enough to handle urban-scale emergency management issues.

The simulated airborne concentration fields on the ground ( $z = 5 \text{ m}$ ) are given in Fig. 5. From 1400 LST to 1600 LST, as the toxic chemical was released continuously, the contaminated region expanded to the north gradually (Figs. 5a–c).

Using the EPA-defined AEGLs values of Piperidine (Table 2) and the method of Stage (2004), the AEGLs values at ground level were also calculated (Fig. 5d). The grids close

to the source location were AEGL-3 (red shading), showing a threat to loss of life, whilst most grids of the contaminated region were of less severity (AEGL-1, AEGL-2) in this numerical experiment.

#### 4.2. The sub-domain-scale numerical experiments

Since not all emergency accidents can reach the urban scale, it is necessary to simulate sub-domain-scale cases using CFD models to improve the planning of prevention and response programs in such environments.

##### 4.2.1. The sub-domain CFD simulation set up

Two sub-domain-scale numerical experiments, whose horizontal resolutions were 10 m and 50 m, were designed to the specifications of Miao et al. (2013). The details of the dimension and grid spacing of the two experiments are presented in Table 3. There were 35 levels in the vertical direction from the ground level to 250 m high for the coarser case (the highest building was 50 m height), and the vertical resolutions of the grids below and above the height of 100 m were set to 5 m and 10 m, respectively. For the 10-m horizontal case (the highest building was 115 m height), 50 levels were set in the vertical direction from the ground level to 450 m high, and a higher vertical grid spacing was used for grids below 150 m high. The inflow conditions (velocity, TKE and its dissipation rate) were set using the inner-domain forecasts of the BJ-RUC system, and the zero-gradient boundary condition was employed at the outflow boundaries (included the top boundary). The no-slip condition was set at the surface of the building, and the wall turbulence functions (Chen et al., 2013) were employed to the grid points adjacent to the walls.

The CFD computational domain images are shown in Fig. 6, whose relative locations in Beijing are indicated in Fig. 1c by two open squares. The buildings’ information for the 10 m horizontal resolution case was obtained by a field survey, while that of the coarser case was estimated by use of Google Earth. The building shapes were simplified to cuboids in this study. Most single buildings cannot be resolved in the coarser computational 3D grid with the 50 m horizontal resolution; therefore, the building heights were set as the estimated average height of the cluster of surrounding buildings. The hypo-

**Table 3.** Grid parameters used for the sub-domain-scale numerical experiments.

Grid Spacing (m)	Dimensions				
	Horizontal	Vertical	X-direction	Y-direction	Z-direction
50	5–10	5–10	130	120	35
10	5–15	5–15	140	140	50

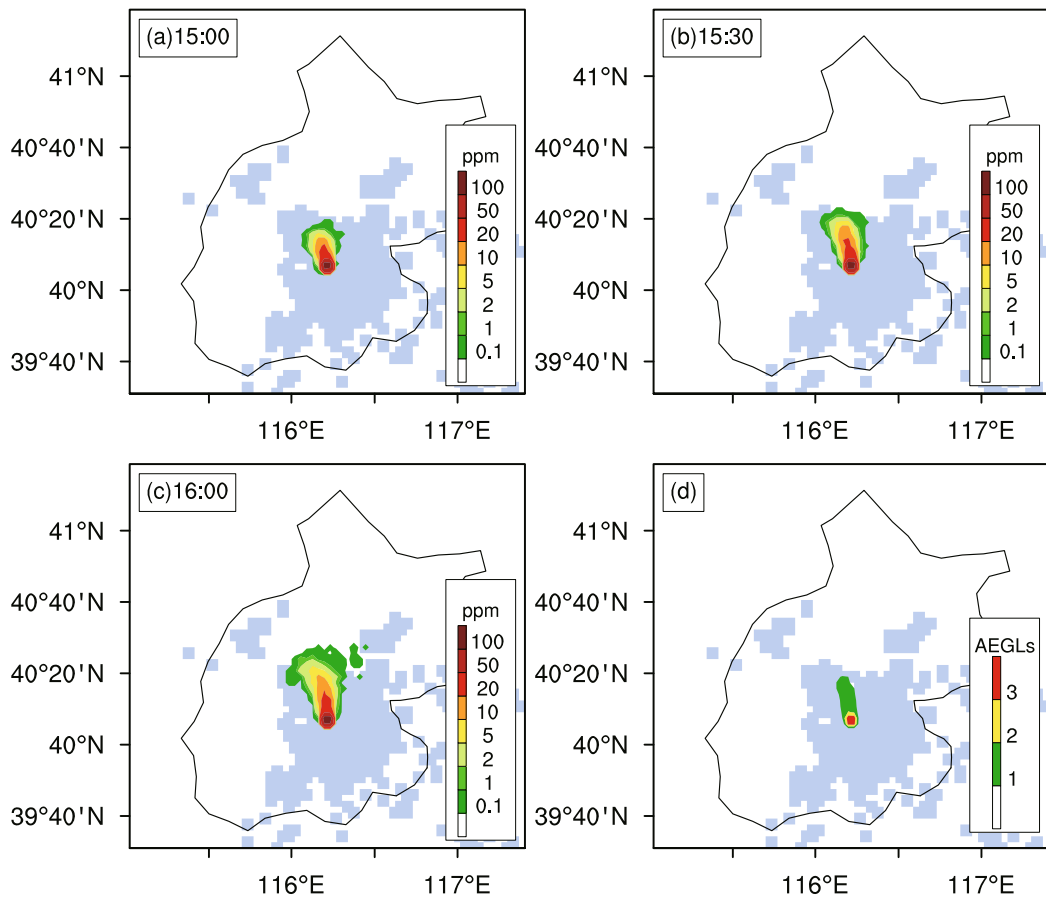


**Fig. 5.** Simulated (a–c) concentrations and (d) AEGLs fields on the ground ( $z = 5$  m): (a) 1500 LST; (b) 1530 LST; (c) 1600 LST. The AEGLs values are calculated using all the simulated results during the whole dispersion period, and the built-up areas of Beijing are indicated by the blue shading. The green (AEGL-1), yellow (AEGL-2) and red (AEGL) shading in (d) indicates increasingly severe adverse effects, i.e., notable discomfort (AEGL-1), serious health effects (AEGL-2), and life threatening effects (AEGL-3).



**Fig. 6.** Google Earth images of the computational domains of the two sub-domain numerical experiments: (a) 50 m horizontal resolution simulation case, indicated by the yellow rectangle; (b) 10 m horizontal resolution simulation case, indicated by the red rectangle.

theoretical exposure periods of these two numerical experiments were both 1 hour, from 1400 LST to 1500 LST (Table 1).

#### 4.2.2. The sub-domain dispersion simulation and hazard evaluation

The OpenFOAM model was firstly driven to recalculate the wind and turbulent fields by using the simulations of the BJ-RUC system. The dispersion process was then simulated by the Lagrangian dispersion model.

Since the simulated results at 1400 LST and 1500 LST had no significant differences, we only present the sub-domain wind vector fields at 1400 LST in Fig. 7. It was found that the wind vectors within the buildings were quite different from the free wind vectors in the boundary regions, which was more obvious in the finer horizontal resolution case (Figs. 7b and 7d).

Comparing the wind fields at different heights, it was found that the impacts of the buildings were more significant at the lower height ( $z = 2.5$  m), which was due to the greater density of buildings at this height. In Fig. 8b, at the height

of 2.5 m, the air flow around building-A was affected by the dense buildings there, resulting in different wind directions and speeds around building-A. This is in comparison to the height of 22.5 m, where the air flow above building-A was more consistent with the inflow (Fig. 8d).

The coarser resolution case (Fig. 7a) seemed to average the configurations of buildings, as well as the wind fields. Therefore in comparison to the 10 m resolution case (Fig. 7b) some small-scale patterns of flow around the buildings were “filtered” in this coarser scale.

Similar to the dispersion numerical experiments at the urban scale, the sources of Piperidine were hypothetically set in the center of buildings at ground level (Fig. 7a and 7b), which were continuously emitting during the simulation period (from 1400 LST to 1500 LST). The ground-level concentration distribution at 1445 LST of the coarser resolution case is given in Fig. 8a. The contaminants were dispersed along building-A and were driven by the local wind into a sector pattern, with some contaminants concentrated at the southeast corner of building-A. The distribution of the AEGLs val-

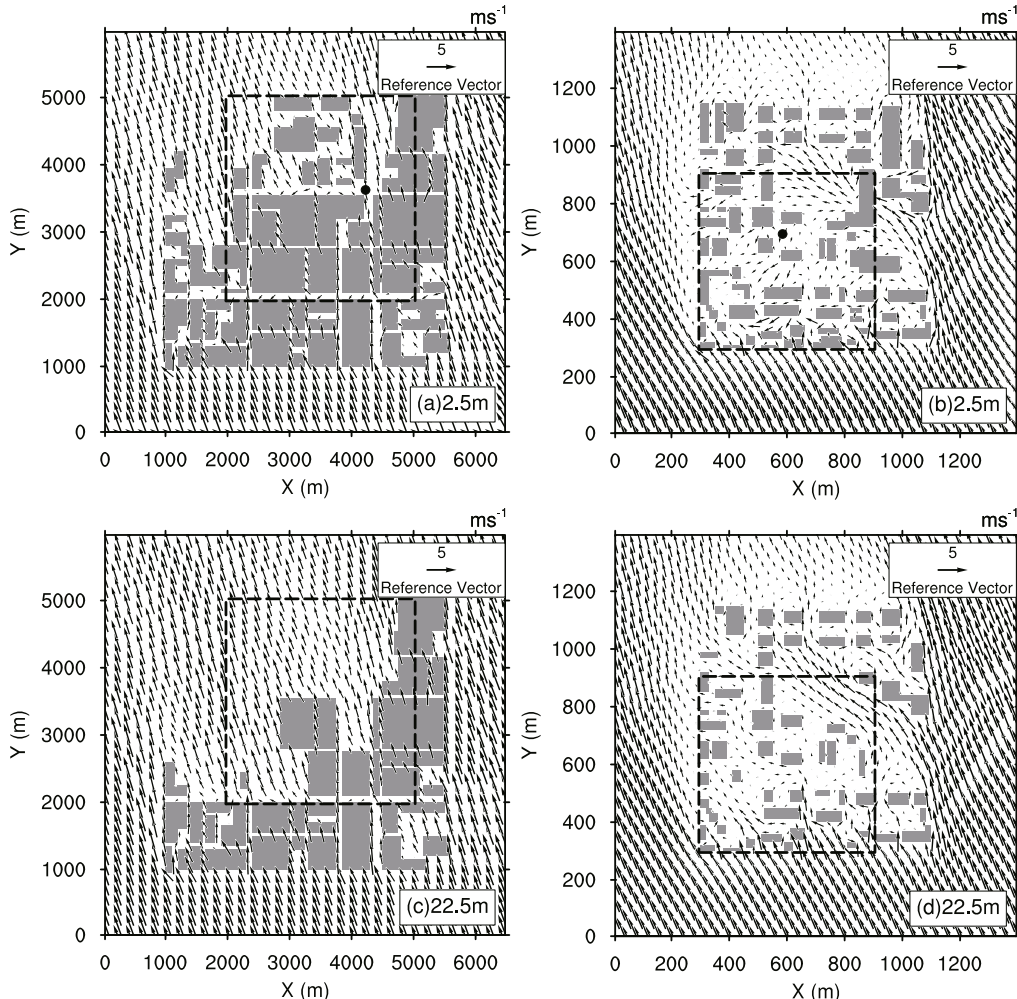


**Fig. 7.** Simulated wind vector fields of the (a, c) 50 m and (b, d) 10 m horizontal resolution cases at 1400 LST for different heights: (a, b) simulations at  $z = 2.5$  m; (c, d) simulations at  $z = 22.5$  m. The dashed line rectangles indicate the regions shown in Figs. 8 and 9.

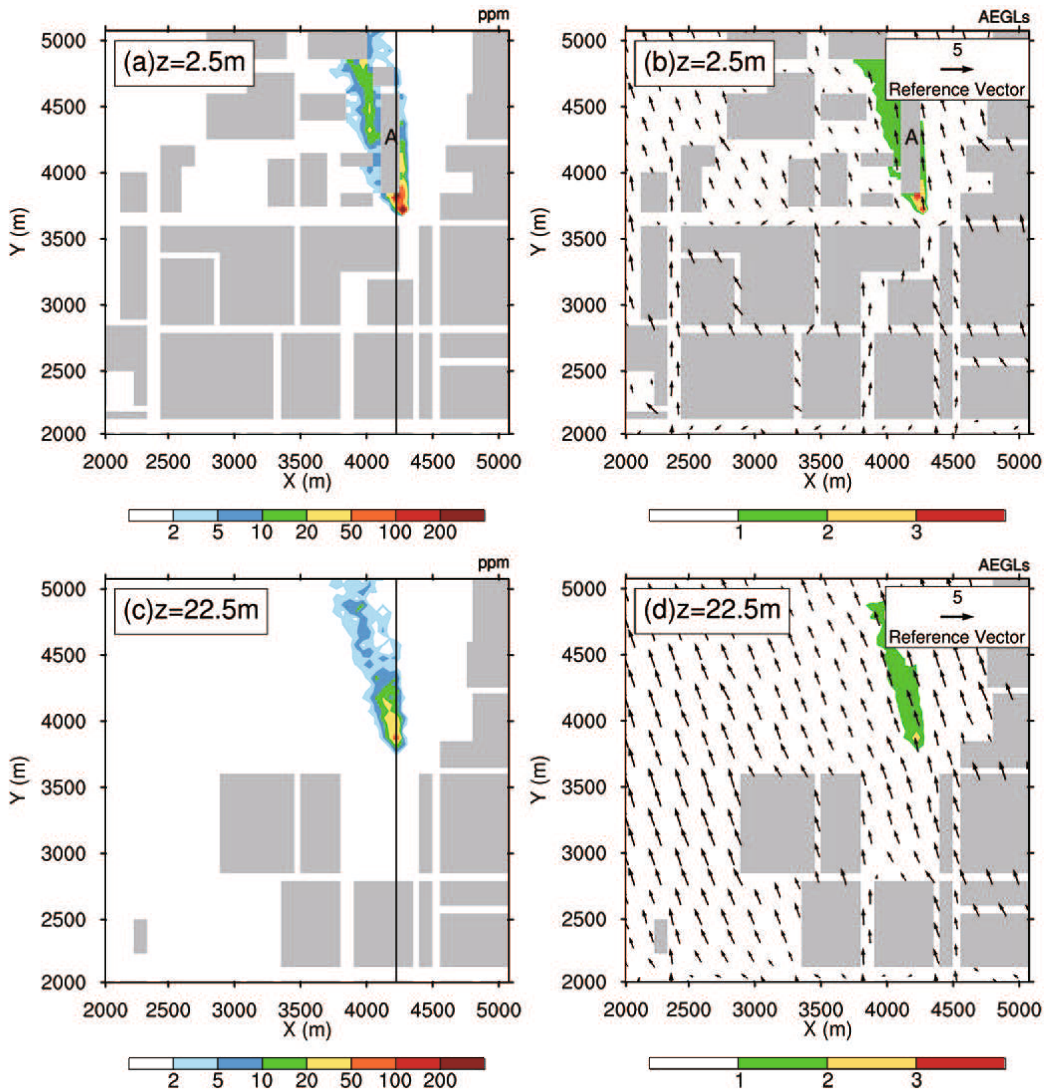


**Fig. 8.** Simulated concentration (ppm) and AEGLs fields of the 50 m horizontal resolution case: (a, c) concentration fields at 1445 LST; (b, d) AEGLs fields. Refer to Fig. 7 for the description of the AEGLs values.

ues was similar to the concentration fields, with the most dangerous region in the southeast corner of building-A (indicated by the red and yellow shading in Fig. 8b).

For the 10 m horizontal resolution case, the local wind fields around the source location (between building-B and building-C) were quite different from the inflow free stream on the inflow boundaries (Figs. 9b and 9d). Here, totally inverted wind vectors were formed, driving toxic contaminants to the south (Fig. 9a). This concentration pattern cannot be easily inferred by the urban-scale simulation. The 10 m AEGLs fields were similar to the concentration fields, and the most dangerous region was calculated to be the street on the west side of building-C with the range  $Y = 600$  m to  $Y = 700$  m (indicated by the red shading in Fig. 9b).

The buildings not only changed the horizontal wind, but also affected the vertical component. The vertical planes of these two sub-domain-scale cases are given in Fig. 10, showing that some vertical vortexes were produced in the canyon formed by the buildings (Fig. 10d). Two clockwise vortexes

were formed on the southern and northern side of building-C (Fig. 10d). The vortex formed between building-B and building-C drove the contaminants to accumulate at the lower northern corner of building-C, and some of the contaminants were transported to a greater height by the updraft flow on the northern side of building-C (Figs. 10c–d). Similar upward transport of contaminants could also be found on the southern side of building-A (Figs. 10a and b). The sub-domain vertical movements within the buildings were affected by the configurations of the buildings and made a difference to the distribution of the concentration, as well as the fields of AEGLs.

## 5. Discussion and conclusions

In this study, a multi-scale atmospheric dispersion model was established by combining the WRF model (the BJ-RUC system), OpenFOAM, and a Lagrangian dispersion model. First, the dispersion model was validated against wind-tunnel experiments. Then, urban- and sub-domain-scale numerical

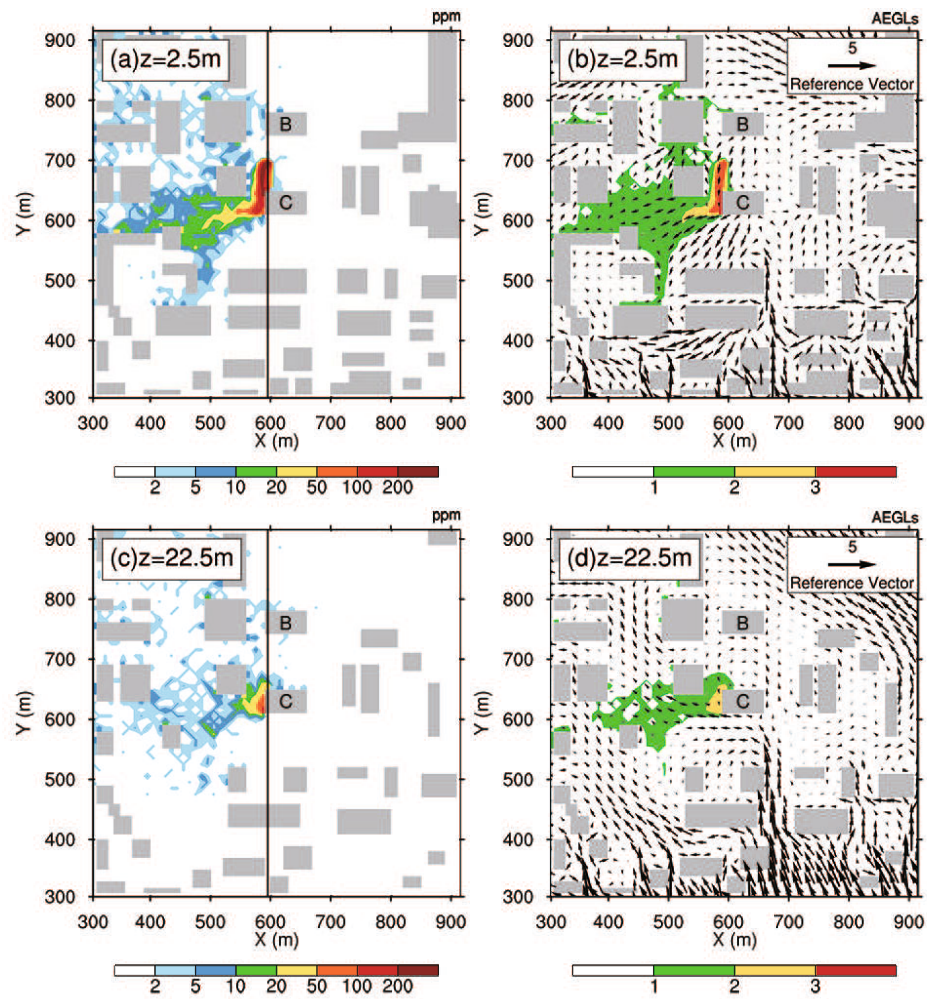


**Fig. 9.** Simulated concentration (ppm) and AEGLs fields of the 10 m horizontal resolution case: (a, c) concentration fields at 1445 LST; (b, d) AEGLs fields. Refer to Fig. 7 for the description of the AEGLs values.

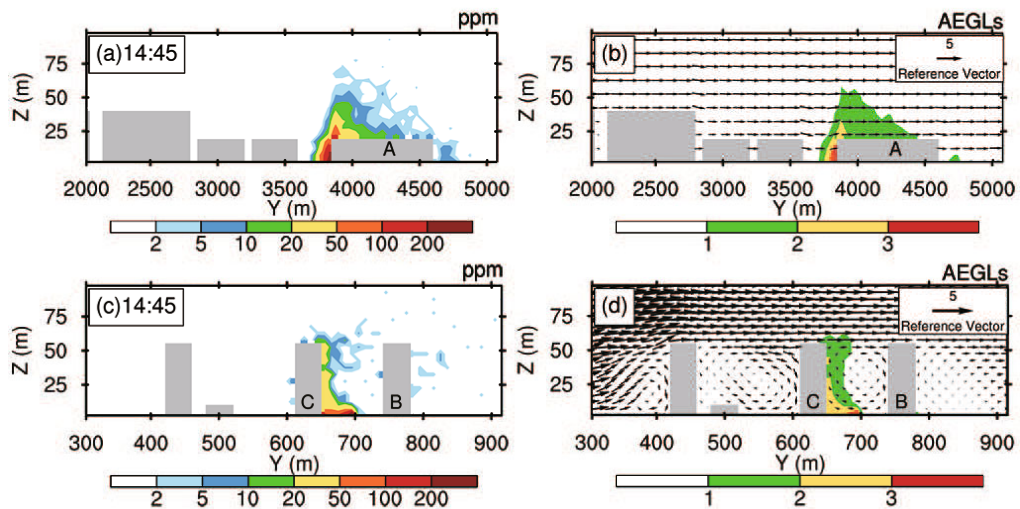


**Fig. 10.** Vertical plane of the concentration fields (ppm) and the AEGLs fields across the black lines in (a, b) Fig. 8 and (c, d) Fig. 9: (a) concentration field at 1445 LST; (b) AEGLs fields of the 50 m horizontal resolution cases; (c) concentration field at 1445 LST; and (d) the AEGLs fields of the 10 m horizontal resolution cases. Refer to Fig. 7 for the description of the AEGLs values in (d).

experiments of a toxic chemical release were performed. The severity levels of these cases were determined by referring to EPA-defined AEGLs values for emergency management.

It was found that the multi-scale atmospheric dispersion model is capable of simulating the flow pattern and concentration distribution on different scales, ranging from several meters to kilometers, i.e., the urban and sub-domain scales.

Using the wind fields from the BJ-RUC system or CFD models, the concentration fields and AEGLs of a point source can be calculated in minutes for any of the scales mentioned above. The multi-scale model can be used as a tool for chemical emergency planning and prevention. The AEGLs results can also be displayed on a Geographic Information System map to give a more comprehensive understanding of the toxic chemical release event.

However, it should be pointed out that CFD models are computationally expensive for sub-domain-scale numerical cases (Fitch et al., 2003). Efforts should be made to develop simplified CFD models for emergency response programs, or establish wind and turbulence libraries for a specific region by pre-computed CFD simulations. In addition, some empirical sub-domain-scale wind field models could be used for emergency management issues, such as Austal2000 (Langner and Klemm, 2011).

Although CFD models can be used to simulate air flow fields with the 50 m horizontal resolution grid, it is noted that some details of buildings and flow fields are lost on this scale. Therefore, it is better to use CFD models to simulate numerical cases with a finer horizontal resolution grid (i.e. 5 m and 10 m), which can resolve most single buildings. However, the horizontal resolution that is employed depends on the specific purpose.

Finally, it should be noted that, although the multi-scale atmospheric dispersion model proposed in this study is for emergency management, it can also be used for urban air quality and planning issues (Fang et al., 2004; Miao et al., 2006, 2013).

**Acknowledgements.** This work was supported by the Public Welfare Special Fund Program (Meteorology) of the Chinese Ministry of Finance (Grant No. GYHY201106033). We thank the Beijing Meteorological Bureau for providing the forecasts of the BJ-RUC system and the observations.

## REFERENCES

- Acuesta, A. D., E. Y. Sanchez, A. Porta, and P. M. Jocovkis, 2011: A method for computing the damage level due to the exposure to an airborne chemical with a time-varying concentration. *Risk Analysis*, **31**(9), 1451–1469.
- Baik, J. J., S. B. Park, and J. J. Kim, 2009: Urban flow and dispersion simulation using a CFD model coupled to a mesoscale model. *J. Appl. Meteor. Climatol.*, **48**, 1667–1681.
- Berrouk, A. S., D. E. Stock, D. Laurence, and J. J. Riley, 2008: Heavy particle dispersion from a point source in turbulent pipe flow. *Int. J. Multiphase Flow*, **34**(10), 916–923.
- Bowonder, B., and T. Miyake, 1988: Managing hazardous facilities: Lessons from the Bhopal accident. *J. Hazard. Mater.*, **19**(3), 237–269.
- Chen, B. C., S. H. Liu, Y. C. Miao, S. Wang, and Y. Li, 2013: Construction and validation of an urban area flow and dispersion model on building scales. *Acta Meteorologica Sinica*, **27**(6), 923–941.
- Fang, X. Y., and Coauthors, 2004: The multi-scale numerical modeling system for research on the relationship between urban planning and meteorological environment. *Adv. Atmos. Sci.*, **21**(1), 103–112, doi: 10.1007/BF02915684.
- Ferziger, J. H., and M. Peric, 2001: *Computational Methods for Fluid Dynamics*. 3rd ed., Springer, 188–202.
- Fitch, J. P., E. Raber, and R. R. Imbro, 2003: Technology challenges in responding to biological or chemical attacks in the civilian sector. *Science*, **302**, 1350–1354.
- Fu, W., H. Fu, K. Skøtt, and M. Yang, 2008: Modeling the spill in the Songhua River after the explosion in the petrochemical plant in Jilin. *Environ. Sci. Pollut. Res.*, **15**(3), 178–181.
- Hanna, S. R., O. R. Hansen, M. Ichard, and D. Strimaitis, 2009: CFD model simulation of dispersion from chlorine railcar release in industrial and urban areas. *Atmos. Environ.*, **43**, 262–270.
- Langner, C., and O. A. Klemm, 2011: A comparison of model performance between AERMOD and AUSTAL2000. *J. Air & Waste Manage. Assoc.*, **61**, 640–646.
- Li, F. Y., J. Bi, L. Huang, C. S. Qu, J. Yang, and Q. M. Bu, 2010: Mapping human vulnerability to chemical accidents in the vicinity of chemical industry parks. *Journal of Hazardous Materials*, **179**, 500–506.
- Li, L., F. Hu, J. Jiang, and X. Cheng, 2007: An application of the RAMS/FLUENT system on the multi-scale numerical simulation of the urban surface layer—A preliminary study. *Adv. Atmos. Sci.*, **24**(2), 271–280, doi: 10.1007/s00376-007-0271-y.
- Miao, S. G., W. M. Jiang, X. Y. Wang, and W. L. Guo, 2006: Impact assessment of urban meteorology and the atmospheric environment using urban sub-domain planning. *Bound.-Layer Meteor.*, **118**, 133–150.
- Miao, Y. C., S. H. Liu, B. C. Chen, B. H. Zhang, S. Wang, and S. Y. Li, 2013: Simulating urban flow and dispersion in Beijing by coupling a CFD model with the WRF model. *Adv. Atmos. Sci.*, **30**(6), 1663–1678, doi: 10.1007/s00376-013-2234-9.
- Miao, Y. C., S. H. Liu, Y. J. Zheng, S. Wang, and Y. Li, 2014: Numerical study of traffic pollutant dispersion within different street canyon configurations. *Adv. Meteor.*, Article ID 458671, doi: 10.1155/2014/458671.
- Okumura, T., N. Takasu, S. Ishimatsu, S. Miyanoki, A. Mitsuhashi, K. Kumada, K. Tanaka, and S. Hinohara, 1996: Report on 640 victims of the Tokyo subway sarin attack. *Annals of Emergency Medicine*, **28**(2), 129–135.
- Santiago, J. L., and F. Martín, 2008: SLP-2D: A new Lagrangian particle model to simulate pollutant dispersion in street canyons. *Atmos. Environ.*, **42**, 3927–3936.
- Stage, S. A., 2004: Determination of acute exposure guideline levels in a dispersion model. *Journal of the Air & Waste Management Association*, **54**, 49–59.
- Stohl, A., C. Foster, A. Frank, P. Seibert, and G. Wotawa, 2005: Technical note: The Lagrangian particle dispersion model FLEXPART version 6.2. *Atmos. Chem. Phys.*, **5**, 2461–2474.
- Tewari, M., H. Kusaka, F. Chen, W. J. Coirier, S. Kim, A. A. Wyszogrodzki, and T. T. Warner, 2010: Impact of coupling a microscale computational fluid dynamics model with a

- mesoscale model on urban scale contaminant transport and dispersion. *Atmospheric Research.*, **96**, 656–664.
- Thompson, R. S., 1993: Building amplification factors for sources near buildings-a wind-tunnel study. *Atmos. Environ.*, **27A** (15), 2313–2325.
- Wang, H., J. Sun, S. Fan, and X. Y. Huang, 2013: Indirect assimilation of radar reflectivity with WRF 3D-Var and its impact on prediction of four summertime convective events. *J. Appl. Meteor. Climatol.*, **52**(4), 889–902.
- Wilson, J. D., and B. L. Sawford, 1996: Review of Lagrangian stochastic models for trajectories in the turbulent atmosphere. *Bound-Layer Meteor.*, **78**, 191–210.
- Zhang, Z., and Q. Chen, 2007: Comparison of the Eulerian and Lagrangian methods for predicting particle transport in enclosed spaces. *Atmos. Environ.*, **41**(25), 5236–5248.